Micelle-Induced Nanofibers

Nanofibers of 1,3-Diphenyl-2-pyrazoline Induced by Cetyltrimethylammonium Bromide Micelles**

Hongbing Fu, Debao Xiao, Jiannian Yao, and Guoqiang Yang*

In recent years, organic nanoparticles (ONPs) of low-molecular-weight (MW) active compounds[1–7] have increasingly become of interest in view of the extensive studies with inorganic colloidal crystals.[8–10] The electronic and optical properties of ONPs are fundamentally different from those of inorganic nanoparticles, because of the presence of van der Waals intermolecular interactions.[11] Furthermore, the orientation of building units in inorganic crystals is identical since atoms can be regarded as hard spheres; in contrast, the stacking mode of organic molecules plays an important role in the properties of ONPs.[4b,6] As far as the application is concerned, the modification of optical and electro-optical properties in ONPs, which are achievable only with particle sizes in the middle or lower nanometer range (50–500 nm), allows much more variability and flexibility in both material synthesis and nanoparticle preparation.[1–7]

Investigations of ONPs, however, are only at their initial stages. Until now, the challenge of synthetically controlling the shape of ONPs has been met with limited success.[5] Herein, we report a self-inducing template growth to produce nanofibers of 1,3-diphenyl-2-pyrazoline (DP) in the presence of cetyltrimethylammonium bromide (CTAB) molecules in an aqueous phase. Firstly, the solubilization of DP molecules into the hydrocarbon core of spherical CTAB micelles induces the sphere-to-rod transition of CTAB micelles; then the induced rodlike CTAB micelles direct the growth of cylindrical DP nanofibers like templates. It is found that the crystal packing forces drive DP molecules self-assembling as J-type aggregates in nanofibers. The concomitant property changes upon the formation of J-type aggregates as well as the natural path to carrier mobility through the fiberlike shape may be explored to enhance device performance in many fields.

Stable DP nanoparticles were prepared by injecting a stock DP/ethanol solution (100 μL, 5.0 mM) to an aqueous micellar solution of CTAB (5 mL) and stirred for 5 minutes. The dispersions of DP nanoparticles into water exhibited an off-white turbidity because of the light scattering of the particles. Interestingly, the morphology of DP particles strongly depends on the concentration of CTAB (C_{CTAB}). Without CTAB molecules in the aqueous phase or C_{CTAB} is less than the first critical micelle concentration (CMC, 0.9 mM), DP molecules would deposit quickly. To elucidate the role played by CTAB molecules, five samples, labeled as **1**–**5**, with $C_{CTAB} = 5.4$, 4.0, 2.7, 1.8 and 0.9 mM, respectively, were used in our experiments.

A first insight into the microscopic structure of DP particles was obtained by field emission scanning electron microscopy (FESEM). Figure 1 illustrates the morphology evolution of DP particles with decreasing C_{CTAB}. At $C_{CTAB} = 5.4$ mM (Figure 1a), only the filter pores are observed, that is, no particles above the pore size exist in sample **1**. At $C_{CTAB} = 4.0$ mM, 20–30 nm particles appear on the millipore filter surface, and partially block the filter pores thus reducing the pore size (Figure 1b). Apparent fiberlike shapes with a width of about 110 nm are identified from the junction between the vaguely seen particles in Figure 1c; moreover, the clearly observed filter pores in this image suggest that almost all particles join in the formation of nanofibers. As the C_{CTAB} decreased further, perfect DP nanofibers form with a diameter of 140 nm at $C_{CTAB} = 1.8$ mM (Figure 1d) and of 225 nm at $C_{CTAB} = 0.9$ mM in (Figure 1e), respectively, while the length of fibers adds up to tens of μm in both cases. Noteworthy, the long rodlike CTAB micelles are observed occasionally by FESEM (the inset in Figure 1a) in the samples with C_{CTAB} about 4.5 mM. This observation provides a clue for us to understand the mechanism of the formation of DP nanofibers, and is discussed below.

Only irregularly deposited CTAB films were observed in the FESEM measurements if we directly dropped and dried

[*] Prof. Dr. J. Yao, Dr. H. Fu, D. Xiao, G. Yang
Center for Molecular Science
Institute of Chemistry
Chinese Academy of Sciences
Beijing 100080 (P.R. China)
Fax: (+86) 10-8261-7315
E-mail: jnyao@mail.iccas.ac.cn

[**] This research was supported in part by the National Natural Foundation of China, the National Research Fund for Fundamental Key Projects No.973 (G19990330) and the Chinese Academy of Sciences.

Supporting information for this article is available on the WWW under http://www.angewandte.org or from the author.

 DOI: 10.1002/ange.200350961

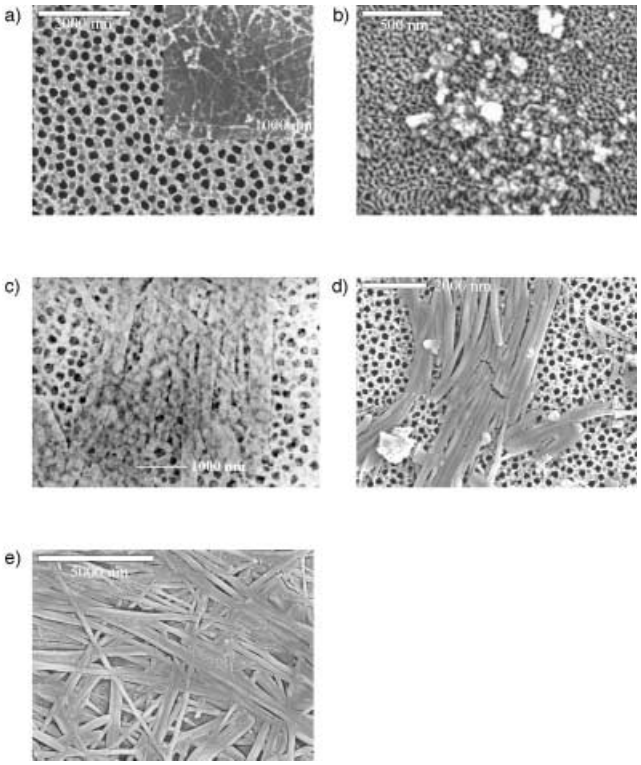

Figure 1. FESEM photographs of DP nanoparticles measured while samples **1**–**5** (image a–e) were filtered on the surface of a millipore filter (pore size 0.02 μm). A gold layer was sputtered onto the surface to increase the conductivity.

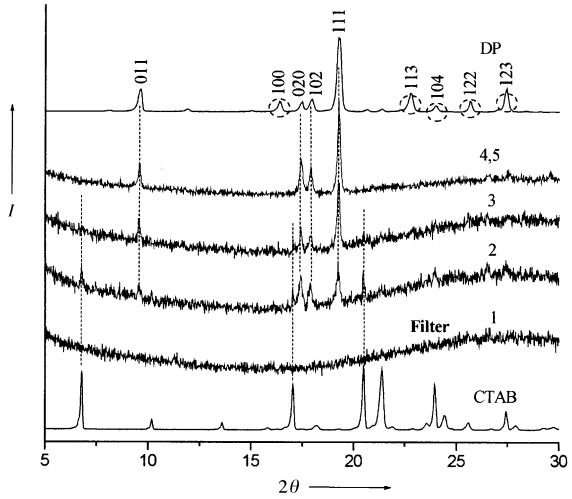

Figure 2. XRD patterns of DP nanoparticles measured while samples **1**–**5** were filtered on the surface of a millipore filter. The top and bottom traces are the spectrum for the pure DP and CTAB powder, I = relative intensity.

the samples on a substrate. Under these conditions, we investigated the DP particles by the means of confocal microscopy based on the strong fluorescence of pyrazoline compounds (see Supporting Information). The fiberlike shapes emerging into the irregular CTAB films were observed while the sample was excited by using a UV light. According to our experiments, these fiberlike DP particles can be reintroduced into water within five to ten minutes under ultrasonic treatment provided we dry the samples under vacuum at $<25\,^{\circ}C$ beforehand. The stability and the facility to redisperse the DP nanofibers account for the thermodynamic stabilization of the colloidal particles by surfactant CTAB molecules.

We also probed the internal structure of DP particles by XRD measurements (Figure 2). Specifically, DP crystallites are in the monoclinic space group $P2_1/c$ with the unit cell dimensions $a = 5.404$, $b = 10.162$, $c = 21.683$ Å, $\beta = 92.85°$, $U = 1189.3$ Å^3, and with $Z = 4$.[12] The characteristic peaks of CTAB attenuate from spectra 2 to 3 and vanish in 5 (Figure 2). This means that the fiberlike particles mainly consist of DP molecules. The intensity ratios between DP characteristic peaks of [111] and [011], $I_{[111]}/I_{[011]}$, are equal to 2.88, 3.14 and 3.74 in the spectra 2, 3 and 4 (or 5), respectively, and is 3.40 in the powder pattern. The concomitant increase of [111] with the growth of nanofibers indicates that DP molecules prefer to arrange themselves along the [111] in the nanofibers. Moreover, peaks of [100], [113], [104], [122] and [123], which are clearly resolved in the DP powder pattern, are not observed in the patterns for the nanofibers. This results from the predominant growth along the [111] plane or the parallel of the incident light to nanofibers placed on the surface of a millipore filter.

Spectroscopic studies, when correlated with the FESEM observations, further clarify the formation process of the fiberlike DP particles. Sample **1** presents a similar absorption spectrum to that of the monomers, including three resolved bands with a maximum at 240 nm arising from the phenyl ring (B_{phenyl}; B = band) and at 302 and 355 nm from the pyrazoline n–π* ($B_{n-\pi^*}$) and π–π* ($B_{\pi-\pi^*}$) transitions,[13] respectively (Figure 3a). We observed the growth of a new band (B_J) at about 425 nm besides the red-shifted B_{phenyl}, $B_{n-\pi^*}$ and $B_{\pi-\pi^*}$ upon going from spectra 2–5 (Figure 3a). This new band of B_J is not detectable in the monomeric solution and is thus expected to originate from the aggregation of DP molecules. The gradual appearance of B_J reflects the formation of DP nanoparticles. To explore the nature of DP aggregates, we also measured the fluorescence emission spectra (Figure 3b). Sample **1** shares the same emission feature of a broad asymmetric band centered at 465 nm with the monomeric solution. From spectra 2 to 5, as the DP molecules aggregate to form nanoparticles, the emission widths gradually become narrower and the emission positions slightly blue shift from 460 to 450 nm. Moreover, the emissions of samples **1**–**5** show a faster fluorescence decay ($\tau = 3.7 \pm 0.3$, 3.4 ± 0.3, 3.1 ± 0.3, 2.5 ± 0.3 and 1.3 ± 0.2 ns, respectively) than that of monomer emission ($\tau = 4.2 \pm 0.3$ ns).

It is known that rodlike CTAB micelles are widely used as templates in the synthesis of inorganic nanorods or nanowires.[8–10] In these cases, C_{CTAB} above the second CMC (100 mM) and/or the introduction of an additional rod-inducing cosurfactant are necessary for the formation of templates of rodlike micelles. Moreover, the diameter of inorganic nanorods or nanowires is determined by the diameter of the rod micelles at the tens-of-nanometer scale. In our experiment, the diameter of DP nanofibers amounts to

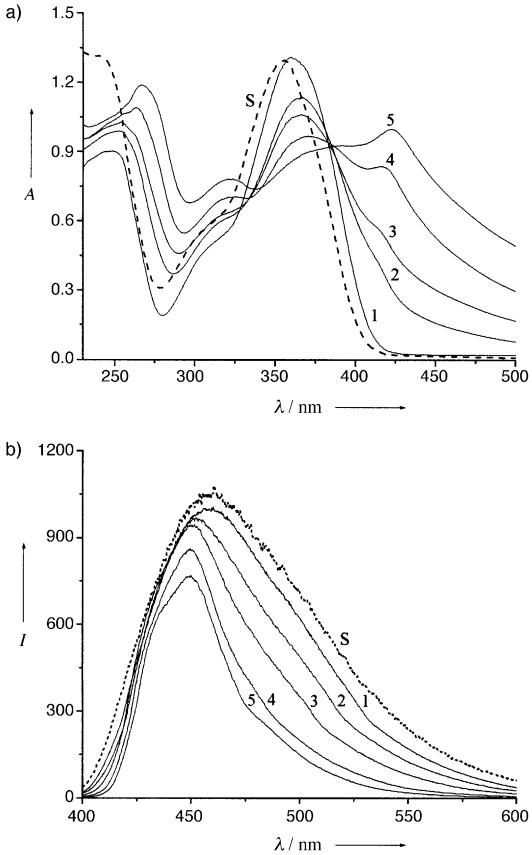

Figure 3. Absorption (a) and emission (b) spectra of samples **1–5** (line 1–5) as compared with the spectrum of 0.1 mM DP/ethanol solution (line S; A = absorbance). Emission spectra were obtained with an excitation wavelength of 360 nm (I = intensity, arbitrary units).

hundreds of nanometer larger than that expected for a rodlike CTAB micelle, and can be tuned easily even at C_{CTAB} within the concentration range of spherical micelles.

CTAB molecules form spherical micelles with a diameter of 6 nm and an aggregation number of 90 within the concentration range from 0.9 to 100 mM.[14] We calculated the molar ratios (N) between DP molecules and CTAB spherical micelles in samples **1–5**, $N = 1.7$, 2.3, 3.3, 5.0 and 10.0, respectively. Analysis of FESEM and spectroscopic data on the parameter N sheds light on the mechanistic basis behind this unusual formation of DP nanofibers.[15] We have identified three distinctive stages in the nanofiber formation (Figure 4). At $N < 2.0$, hyrophobic DP molecules dissolve in the spherical CTAB micelles because of a process called solubilization.[16] In Figure 3, the optical absorption and emission of sample **1** ($N = 1.7$) is similar to that of the monomer. That is, DP molecules which dissolve into spherical CTAB micelles are separated from each other by the CTAB alkyl chains, and therefore in a monomeric state. Importantly, DP molecules, which dissolve into spherical CTAB micelles, induce the sphere-to-rod transition of CTAB micelles like a rod-inducing reagent, such as sodium salicylate[17] and aromatic hydrocarbons.[18] Indeed, such rodlike CTAB micelles were observed by FESEM (Figure 1a inset and Supporting Information). The sphere-to-rod transition of CTAB micelles occurs in our systems at $N \approx 2.0$. At this molar ration, each spherical CTAB micelle will dissolve more than two DP molecules, the strong π–π interactions between DP molecules are likely to drive them to aggregate with each other. Furthermore, the formed rodlike micelles act as templates directing the growth of DP nanofibers. The layer of CTAB molecules surrounding the core of DP provides excellent colloidal stability of the nanofibers. The diameter of DP nanofibers could be easily tuned by changing the value of N.

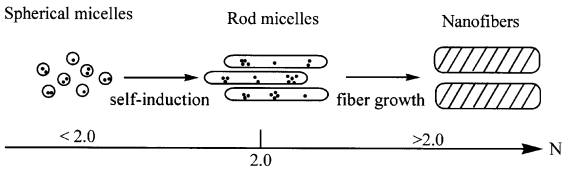

Figure 4. Cartoon representation of self-inducing templates growth for DP nanofibers.

The spectral characteristics observed for DP nanoparticles as compared with those of monomers, that is, the red-shifted absorption, the smaller Stokes shift, and the fast fluorescence decay, are quite different from our previous study on spherical nanoparticles of 1-phenyl-3-((dimethylamino)styryl)-5-((dimethylamino)phenyl)-2-pyrazoline (PDDP),[4a] in which the nanoparticle emission shifts to a lower energy and decays slower than PDDP monomer emission does. In fact, the optical features of DP aggregates are consistent with a picture of J aggregation.[19] According to the molecular exciton model,[19c] the stacking angle, α, which defines the angle between the transition dipole and the molecular axis of the aggregate, is 54.7° or less in a J-type aggregate. As there is no substituent at the 5-position the DP molecules are planar, which leads to a closely packed crystal structure in $P21/c$.[12] The stacking angle between the transition dipole of the DP molecule and the crystallographic a axis is calculated to be 50.7°,[20] which is less than 54.7° and also consistent with the model of J aggregate.[19] The perpendicular distance between two adjacent molecules along the crystallographic a axis is about 3.6 Å.[12] As confirmed by XRD measurements, DP molecules prefer to grow along the [111] plane in nanofibers. Therefore, it is the crystal packing forces that drive theself-assembly of DP molecules as J-type aggregates in DP nanofibers.

In summary, we have developed a simple solution method, self-inducing template growth, for the preparation of stable DP nanofibers in the presence of CTAB in aqueous phase. On the one hand, the surfactant CTAB molecules assume the role of surface-active colloidal stabilizers. On the other hand, those DP molecules dissolved in spherical CTAB micelles induce the formation of rodlike CTAB micelles, and then the as formed rod micelles direct the growth of cylindrical DP nanofibers like templates. It is found that DP nanofibers predominantly grow along the [111], and the crystal packing forces drive DP molecules self-assembling as J-type aggregates in nanofibers.

Received: January 17, 2003 [Z50961]

Keywords: aggregation · micelles · nanostructures · photochemistry · pi interactions

[1] H. Kasai, H. S. Nalwa, H. Oikawa, S. Okada, H. Matsuda, N. Minami, A. Kakuta, K. Ono, A. Mukoh, H. Nakanishi, *Jpn. J. Appl. Phys. Part 2* **1992**, *31*, L1132.
[2] A. Ibanez, S. Maximov, A. Guiu, C. Chaillout, P. L. Baldeck, *Adv. Mater.* **1998**, *10*, 1540.
[3] D. Horn, J. Rieger, *Angew. Chem.* **2001**, *113*, 4460; *Angew. Chem. Int. Ed.* **2001**, *40*, 4331.
[4] a) H. B. Fu, J. N. Yao, *J. Am. Chem. Soc.* **2001**, *123*, 1434; b) H. B. Fu, B. H. Loo, D. B. Xiao, R. M. Xie, X. H. Ji, J. N. Yao, B. W. Zhang, L. Q. Zhang, *Angew. Chem.* **2002**, *114*, 1004; *Angew. Chem. Int. Ed.* **2002**, *41*, 962; c) R. M. Xie, D. B. Xiao, H. B. Fu, X. H. Ji, W. S. Yang, J. N. Yao, *New J. Chem.* **2001**, *25*, 1362.
[5] J. K. Lee, W. K. Koh, W. S. Chae, Y. R. Kim, *Chem. Commun.* **2002**, 138.
[6] B. K. An, S. K. Kwon, S. D. Jung, S. Y. Park, *J. Am. Chem. Soc.* **2002**, *124*, 14410.
[7] X. C. Gong, T. Milic, C. Xu, J. D. Batteas, C. M. Drain, *J. Am. Chem. Soc.* **2002**, *124*, 14290.
[8] X. G. Peng, L. Manna, W. D. Yang, J. Wichham, E. Scher, A. Kadavanich, A. P. Alivisatos, *Nature* **2000**, *404*, 59.
[9] a) Y. Y. Yu, S. S. Chang, C. L. Lee, C. R. C. Wang, *J. Phys. Chem. B* **1997**, *101*, 6661; b) S. Link, M. B. Mohamed, M. A. El-Sayed, *J. Phys. Chem. B* **1999**, *103*, 3073.
[10] a) N. R. Jana, C. J. Murphy, *Chem. Commun.* **2001**, 617; b) C. J. Murphy, N. R. Jana, *Adv. Mater.* **2002**, *14*, 80.
[11] a) Silinsh, E. A. *Organic Molecular Crystals: Their Electronic States*; Springer-Verlag: Berlin, **1980**; b) M. Pope, C. E. Swenberg, *Electronic Processes in Organic Crystals*; Oxford Univ. Press: Oxford, **1982**.
[12] B. Duffin, *Acta Crystallogr. Sect. B* **1968**, *24*, 1256.
[13] F. Wilkinson, G. P. Kelly, C. Michael, *J. Photochem. Photobiol. A* **1990**, *52*, 309.
[14] T. Imae, R. Kamiya, S. Ikeda, *J. Colloid Interface Sci.* **1985**, *108*, 215.
[15] Tuning the value of *N* by varying the injected quantity of DP/ethanol stock solution could obtain the same results. Moreover, stepwise injection also produced nanofibers.
[16] *Solubilization in Surfactant Aggregates* (Eds.: S. D. Christian, F. F. Scamehorn), Marcel Dekker, New York, **1995**.
[17] T. Shikata, H. Hirata, T. Kotaka, *Langmuir* **1988**, *4*, 354.
[18] P. Lianos, J. Lang, C. Strazielle, R. Zana, *J. Phys. Chem.* **1982**, *86*, 1019.
[19] a) S. Özçelik, D. L. Akins, *J. Phys. Chem. B* **1999**, *103*, 8926–8929; b) E. S. Emerson, M. A. Conlin, A. E. Rosenoff, K. S. Norland, H. Rodriguez, D. Chin, G. R. Bird, *J. Phys. Chem.* **1967**, *71*, 2396; c) M. Kasha, H. R. Rawls, M. A. El-Bayoumi, *Pure Appl. Chem.* **1965**, *11*, 371.
[20] The angle between the pyrazoline plane and the crystallographic *a* axis is calculated to be 53.52°.[12] Thus, $\alpha = 53.52° - (\beta - 90°) \approx 50.7°$.

